

Optical spectroscopy of X-MEGA targets

I. CPD -59° 2635: A New Double-Lined O type Binary in the Carina Nebula

J.F. Albacete Colombo^{1*} †, N.I. Morrell^{1*} ‡ §, V.S. Niemela^{1*} ¶ and M.F. Corcoran^{2,3}

¹ *Facultad de Ciencias Astronómicas y Geofísicas, Universidad Nacional de La Plata, Paseo del Bosque S/N, 1900 La Plata, Argentina*

² *Universities Space Research Association, 7501 Forbes Blvd, Ste 206, Seabrook, MD 20706, USA*

³ *Laboratory for High Energy Astrophysics, Goddard Space Flight Center, Greenbelt MD 20771, USA*

22 October 2018

ABSTRACT

Optical spectroscopy of CPD -59° 2635, one of the O-type stars in the open cluster Trumpler 16 in the Carina Nebula, reveals this star to be a double-lined binary system. We have obtained the first radial velocity orbit for this system, consisting of a circular solution with a period of 2.2999 days and semi amplitudes of 208 and 273 km s⁻¹. This results in minimum masses of 15 and 11 M_⊙ for the binary components of CPD-59° 2635, which we classified as O8V and O9.5V, though spectral type variations of the order of 1 subclass, that we identify as the *Struve-Sahade effect*, seem to be present in both components. From ROSAT HRI observations of CPD-59° 2635 we determine a luminosity ratio $\log(L_x/L_{bol}) \approx -7$, which is similar to that observed for other O-type stars in the Carina Nebula region. No evidence of light variations is present in the available optical or X-rays data sets.

Key words: open clusters and associations: individual (Trumpler 16) – stars: binaries – early-type – stars: individual (CPD -59° 2635) – X-rays: stars

1 INTRODUCTION

The very young Carina Nebula region contains several open clusters with a rich population of O-type stars. Among them, Trumpler 16 is one of the most conspicuous. One of its members, CPD -59° 2635 ($V=9.27$, $\alpha_{2000}=10^\circ 45' 12.78''$, $\delta_{2000}=-59^\circ 44' 46.6''$; Massey & Johnson, 1993) has been observed in the context of the international X-Mega campaign, which involves optical spectroscopy of OB stars showing X-ray emission on ROSAT-HRI images (Corcoran 1999) || CPD-59° 2635 is one of the OB stars in the neighborhood of η Car-

inae also detected as a bright X-ray source. Figure 1 shows an X-ray image centered on CPD -59° 2635 obtained through combination of 3 deep *ROSAT* HRI pointings (see below) along with the optical field from the Digitized Sky Survey.

Because a massive binary system could influence its emergent X-ray flux as a result of colliding stellar winds (e.g. Chlebowski & Garmany, 1991), it is important to verify the frequency of close multiple systems among the Carina OB stars which are detected as X-ray sources. We wonder, for example, if wind collision might be the physical reason that makes CPD -59° 2635 brighter in X-rays than its close neighbor HD 93343 very similar in both visual brightness and spectral type (see Fig. 1).

CPD -59° 2635 has received different designations in the literature. The IDS catalogue (Jeffers et al. 1963) refers to it as IDS 10452 S 5946 as possibly forming a visual binary with HD 93343, of similar V magnitude, about 14" to the South. Stephenson & Sanduleak (1971) gave to CPD -59° 2635 the number 1872 in their catalogue of “Luminous Stars in the Southern Milky Way” (LSS), but misleadingly providing the cross-identification as “HD 93343?”. Feinstein et al. (1973) assigned to CPD -59° 2635 the number 34, among the probable members of the open cluster Trumpler 16.

* Visiting Astronomer, CASLEO, operated under agreement between CONICET and National Universities of La Plata, Córdoba and San Juan, Argentina.

† Fellow of CIC, Prov. de Buenos Aires, Argentina.

‡ Visiting Astronomer, CTIO, NOAO, operated by AURA Inc., for NSF.

§ Member of Carrera del Investigador Científico, CONICET, Argentina.

¶ Member of Carrera del Investigador Científico, CIC, Prov. de Buenos Aires, Argentina.

|| (See <http://lheawww.gsfc.nasa.gov/users/corcoran/xmega/> for a more comprehensive description of the X-Mega campaign).

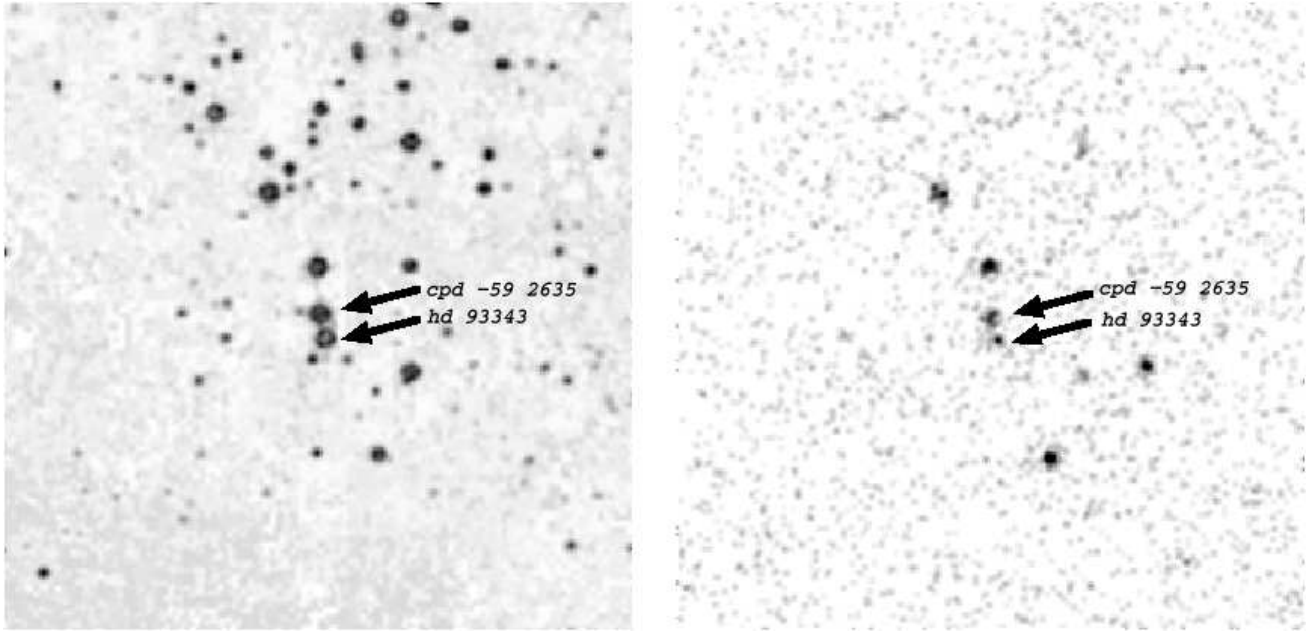


Figure 1. Optical field around CPD $-59^{\circ} 2635$ (left) from digitized sky survey and *ROSAT* HRI image (right). The fields of view are $6' \times 6'$.

2 OBSERVATIONS

Our observations consist of optical spectrograms of CPD $-59^{\circ} 2635$, obtained during 1984 at Cerro Tololo Interamerican Observatory (CTIO), Chile, and between 1997 and 2000 at Complejo Astronómico El Leoncito (CASLEO).

The first set of 11 observations was obtained in March 1984 at CTIO using the Carnegie Image Tube Spectrograph (CTIS) attached to the 1-m Yale telescope. These spectrograms, covering a wavelength range from 3900 to 4900 Å at a reciprocal dispersion of 43 Å mm^{-1} were widened to 1 mm and secured on Kodak IIIa-J baked emulsion. A He-A lamp was used as a comparison source. These photographic spectrograms were digitized with a Grant micro-densitometer at La Plata Observatory, and subsequently analyzed with IRAF ^{**} routines.

Spectral CCD images of CPD $-59^{\circ} 2635$ were obtained at CASLEO observatory, between January 1997 and June 2000 with the 2.15-m Jorge Sahade telescope, mainly as part of the observations for the X-Mega campaign. We used a REOSC echelle Cassegrain spectrograph and a Tek 1024 \times 1024 pixels CCD as detector to obtain 27 spectra in the wavelength range from 3500 to 6000 Å at a reciprocal dispersion of 0.17 Å px^{-1} at 4500 Å. The S/N of these data is ~ 110 (although it changes, of course, with position within each echelle order).

Four additional observations were obtained at CASLEO with a Boller & Chivens (B&C) spectrograph attached to the 2.15m telescope, using a PM 516 \times 516 pixels CCD as detector, and a 600 l mm^{-1} diffraction grating, yielding a reciprocal dispersion of 2.5 Å px^{-1} . These spectra cover the spectral range from ~ 3800 to 4900 Å, and their S/N is ~ 300 . One more spectrum of CPD $-59^{\circ} 2635$ was obtained

at CASLEO with the REOSC spectrograph in its simple dispersion mode, using a 600 l mm^{-1} grating and the Tek 1024 \times 1024 CCD as detector, at a resulting reciprocal dispersion of 1.8 Å px^{-1} . The central wavelength of this observation is 4700 Å and the corresponding S/N is ~ 300 .

The usual series of bias, flat field and dark exposures were also secured during each observing night for every CCD data set. The CCD images were processed and analyzed with IRAF routines at La Plata Observatory.

3 RESULTS AND THEIR DISCUSSION

3.1 Radial Velocity orbit of CPD $-59^{\circ} 2635$

A first inspection of our high resolution echelle spectrograms revealed double lines present in some of them, indicating that CPD $-59^{\circ} 2635$ was probably a double-lined spectroscopic binary. Figure 2 shows the behavior of He II 4686 Å line in echelle spectra of CPD $-59^{\circ} 2635$, obtained at different observing dates.

Radial velocities were determined from our spectra of CPD $-59^{\circ} 2635$, fitting Gaussian profiles to the absorption lines.

We used for radial velocity determination several lines of He I along with He II 4686 Å which appear as the least affected by pair blending. The Pickering (4-n) series of He II absorptions of the two binary components are not well resolved in our spectra, these lines being broader than other He II and He I absorptions. We interpret this fact as indicative of higher pressure broadening acting in the region where these lines form, which must be deeper in the atmosphere than the formation region of He I lines. As a consequence, these (4-n) series lines are more seriously blended than the other absorptions in the spectrum of CPD $-59^{\circ} 2635$ and we decided not to include them in the average radial velocities presented in Table 1. We also derived radial velocities from

^{**} Image Reduction and Analysis Facility, distributed by NOAO, operated by AURA, Inc., under agreement with NSF.

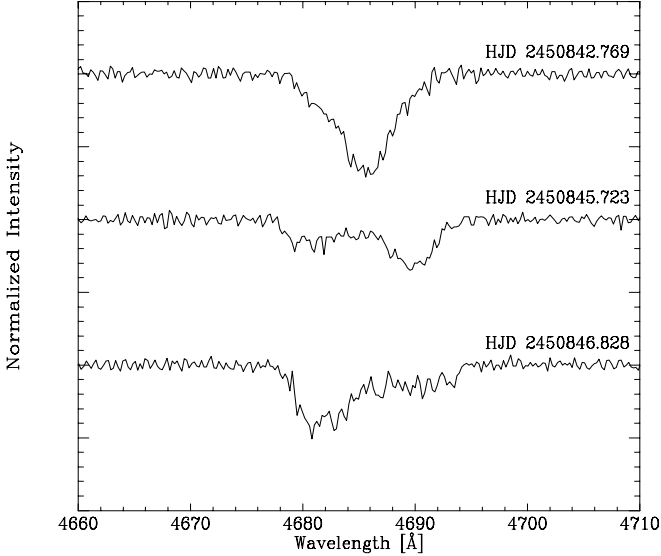


Figure 2. HeII 4686 Å absorption in the spectrum of CPD -59° 2635 at different observing dates, showing the doubling of spectral lines.

our lower resolution, but higher S/N CCD spectra and from our digitized photographic plates. The radial velocities were computed as unweighted mean values of individual velocities determined for each spectral line.

The journal of our radial velocity observations is presented in Table 1. In successive columns, we quote the Heliocentric Julian Date (HJD), the corresponding orbital phase (as explained below), the measured average radial velocities for the primary and secondary components, and their standard deviations (s.d.). We identified the primary component as the one having deeper absorptions of HeII lines.

From the radial velocities listed in Table 1, it was already apparent that the orbital period of CPD-59° 2635 was of the order of a few days. A period search routine based on the modified Lafler & Kinman (1965) method (Cincotta, Méndez & Nuñez 1995) applied to all the radial velocity observations of the primary component of CPD-59° 2635 as listed in Table 1, yielded as the most probable period $P = 2.29995 \pm 0.00002$ days. Initial orbital elements were estimated, leaving also the period as a free parameter, resulting in an orbital solution of negligible eccentricity ($e = 0.005 \pm 0.008$) with no significant change in the orbital period. We therefore considered the orbit to be circular, and the above mentioned value of the period to be the most probable, and proceeded to find the best fit for the remaining orbital parameters. In order to avoid as much as possible pair blending effects, we computed the orbital elements of CPD-59° 2635 using only radial velocities derived from our high resolution observations of both binary components, obtained at the orbital phase intervals 0.1 to 0.4 and 0.6 to 0.9, of the binary period. The resulting orbital elements are listed in Table 2.

Figure 3 represents the complete set of observed radial velocities as a function of the adopted orbital period, along with the circular orbital solution from Table 2.

Table 1. Radial-velocity measurements for CPD -59° 2635.

HJD 2400000+	phase ϕ	Primary $km\ s^{-1}$	s.d. $km\ s^{-1}$	Secondary $km\ s^{-1}$	s.d. $km\ s^{-1}$
45776.826†	0.86	193	34	-132	56
45777.783†	0.27	-214	56	+256	41
45778.731†	0.63	+179	22	-210	28
45779.715†	0.11	-138	25	+160	10
45780.748†	0.56	+27	25	—	—
45781.644†	0.95	+37	28	—	—
45782.730†	0.42	-116	46	+98	28
45783.677†	0.84	+175	25	-223	61
45784.682†	0.27	-204	47	+219	68
45785.634†	0.62	+181	27	-210	30
45786.623†	0.12	-135	28	+180	34
50495.835	0.64	+163	23	-225	18
50498.826	0.92	+108	10	-131	18
50506.834	0.43	-68	19	+132	13
50841.793	0.07	-86	27	+152	28
50842.769	0.49	+3	9	—	—
50843.727	0.91	+132	18	-143	16
50844.718	0.34	-168	10	+236	29
50845.723	0.77	+205	11	-271	37
50846.828	0.26	-202	27	+270	21
50847.649	0.61	+150	10	-184	35
50848.779	0.10	-133	12	+189	24
50850.724	0.95	+86	17	-101	18
50851.655	0.35	-162	17	+231	24
50852.828	0.89	+177	19	-191	18
50859.789‡	0.61	+112	21	—	—
50861.781‡	0.76	+189	24	-248	25
50862.762‡	0.18	-192	18	+243	33
50868.714‡	0.77	+188	22	—	—
51208.709	0.61	+134	17	-214	21
51209.714	0.04	-49	27	—	—
51210.727	0.47	-36	18	—	—
51211.715	0.90	+118	6	-179	24
51215.682	0.63	+137	17	-197	17
51216.653	0.05	-82	20	+80	12
51217.673	0.49	-12	21	—	—
51218.632	0.91	+109	32	-149	37
51712.448	0.62	+136	20	-193	30
51712.478	0.63	+179	56	—	—
51715.463	0.93	+84	16	-120	10
51716.483	0.37	-165	33	184	19
51716.521	0.39	-131	16	160	23
51718.555‡	0.27	-220	59	220	31

NOTE: Orbital phases have been calculated with ephemeris of table 2. † indicates the lower resolution observations obtained with the CITS, and ‡ those obtained either with the B&C spectrograph or the REOSC spectrograph in simple dispersion mode.

3.2 Spectral classification of the binary components of CPD -59° 2635.

CPD-59° 2635 has been previously classified by Walborn (1982) as O7Vnn; and by Levato & Malaroda (1982) as O8/9:V “+ companion?”, already pointing out its probable binary nature. Massey & Johnson (1993) classified CPD-59° 2635 as O8.5V. The spectrum of CPD-59° 2635 (identified as star number 516), shown in the last mentioned paper displays indeed double lines, apparently not noticed by the authors.

Two spectra of CPD-59° 2635 from our lower resolu-

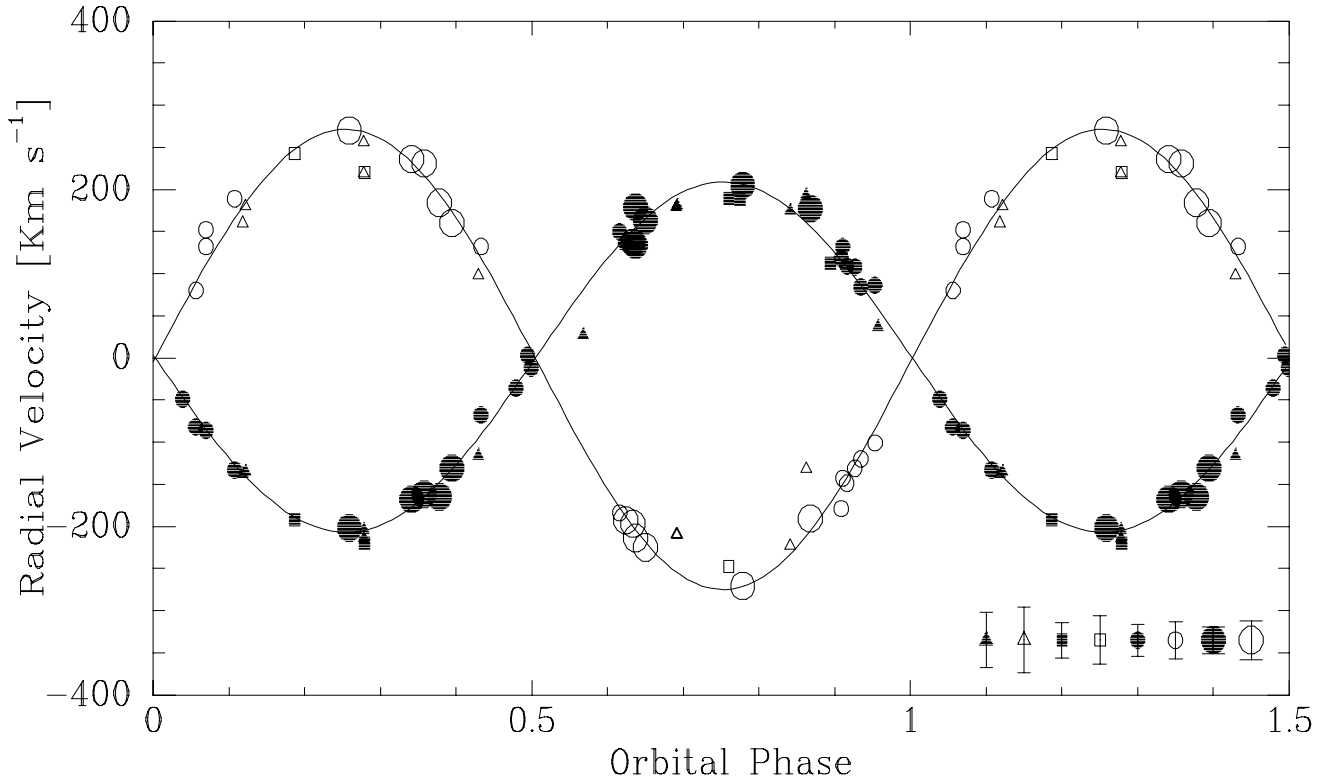


Figure 3. Radial velocity orbit for CPD -59° 2635. The meaning of the symbols is as follows: *filled and open* symbols refer to the primary and secondary stars, respectively. *Circles* represent REOSC-echelle spectra (bigger symbols refer to data used in the calculation of the orbital solution); *squares* stand for B&C and REOSC-DS spectra and *triangles*, for CITS spectra. Typical error bars for each data-set are also indicated.

Table 2. Circular orbital elements of CPD -59° 2635.

P [days]	$2.29995 \pm 2 \times 10^{-5}$
K_1 [$km\ s^{-1}$]	208 ± 2
K_2 [$km\ s^{-1}$]	273 ± 2
γ [$km\ s^{-1}$]	0 ± 1
T_{max} [HJD]	2450845.664 ± 0.01
$a_1 \cdot \sin i$ [R_\odot]	9.4 ± 0.1
$a_2 \cdot \sin i$ [R_\odot]	12.4 ± 0.1
$M_1 \sin^3 i$ [M_\odot]	15.0 ± 0.5
$M_2 \sin^3 i$ [M_\odot]	11.4 ± 0.5
$q(M_2/M_1)$	0.76 ± 0.01

NOTE: T_{max} represents the time of maximum radial velocity of the primary component.

tion CCD images, corresponding to nearly opposite binary phases, are illustrated in Figure 4, where a difference in the relative intensities of HeI 4471Å and HeII 4542Å is evident. In the upper spectrum shown in Figure 4, obtained at binary phase 0.76P, HeI and HeII absorptions appear similar indicating a spectral type O7; while in the lower spectrum, obtained at the binary phase 0.18P, HeI absorption is clearly stronger than that of HeII, corresponding to a spectral type O8-9. Such spectral variations might explain the slightly different classifications given to this star by different authors.

Keeping in mind the known difficulties in classifying spectra of close binaries, and the above illustrated spectral variations, we have nevertheless tried to estimate the spectral types of the binary components of CPD -59° 2635.

An inspection of our high and intermediate resolution

observations showed that both stars present absorption-line ratios of HeI/HeII ≥ 1 , indicating spectral types probably later than O7. From the spectra with maximum separation of the lines of the binary components, and using the classification criteria described by Walborn & Fitzpatrick (1990), we derived spectral types of O8:V and O9.5:V for the primary and secondary components, respectively.

In order to provide an additional estimate for the spectral types of the binary components of CPD -59° 2635, we considered the HeI(4922)/HeII(5411) ratio, following the classification criteria proposed by Kerton et al. (1999). The equivalent widths (W) of the 5411 Å and 4922 Å lines were measured in normalized spectra, by means of a Gaussian fit to the absorption profiles, though HeII 5411 Å looks somewhat blended even at phases of maximum radial velocity separation (as above discussed) which causes less confident W determinations. We found equivalent width ratios $R(W_{4922}/W_{5411})$ of 0.54 ± 0.03 and 1.18 ± 0.04 for the primary and secondary components, respectively, corresponding to spectral types of O8V and O9.5V, with some variations depending probably on binary phase.

Figure 5 shows the spectral region comprising HeI 4922 Å and HeII 5411 Å lines on echelle spectrograms of CPD -59° 2635 near the phases of maximum separation of the components.

By inspection of the HeI and HeII spectral lines observed during different phases of the binary motion, we found line depth variations that can be appreciated in Figures 2 and 5. We identify this phenomenon as the *Struve-Sahade effect* (cf. Gies et al. 1997 and references therein) observed in

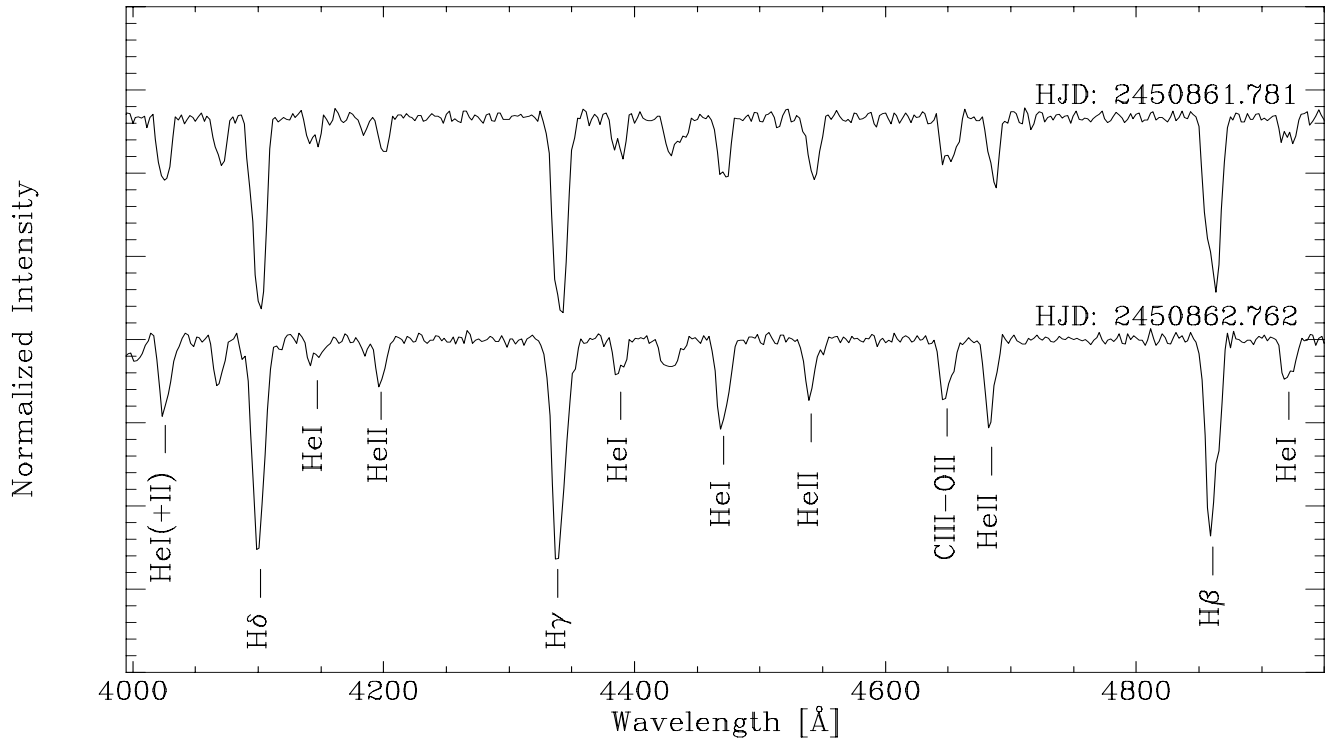


Figure 4. Spectra of CPD -59° 2635 obtained at CASLEO with the B&C spectrograph. Spectral features marked are: H Balmer lines, HeI(+II) 4026 Å, HeI 4143 Å, HeII 4200 Å, HeI 4388 Å, HeI 4471 Å, HeII 4541 Å, CIII + OII 4650 Å blend, HeII 4686 Å, HeI 4713 Å, and HeI 4921 Å. Note the difference in relative intensities of HeI 4471Å and HeII 4541Å between both spectra.

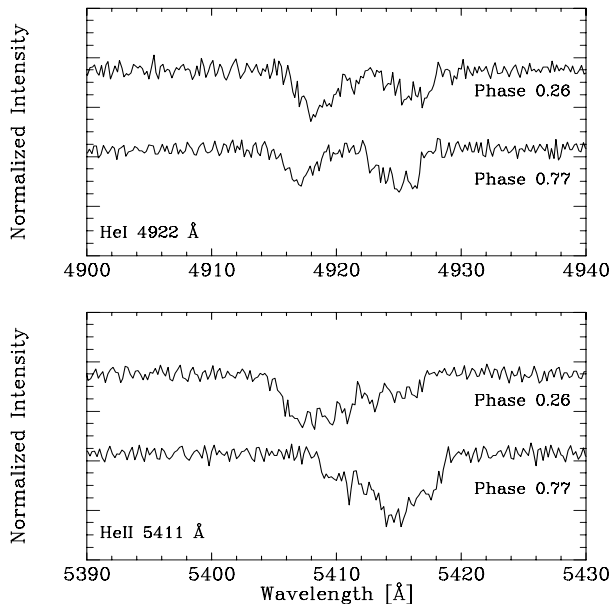


Figure 5. HeI 4922 Å and HeII 5411 Å lines in the spectrum of CPD -59° 2635 at phases 0.26 and 0.77

massive close binaries, which consists in the deepening of the spectral lines of the secondary star when it approaches to the observer. In our spectra, variable line depths seem to be present in both binary components although stronger variations are observed in the secondary star.

Applying again the classification criteria proposed by

Kerton et al. (1999) we found variations around one subclass in spectral types for both binary components, going from O7 to O8 for the primary and O8.5 to O9.5 for the secondary star. However, the errors involved in the EW measurements (especially those affecting the HeII 5411 Å line) are also considerable and, as a consequence, we cannot address any conclusive statement about the phase dependence of these variations until higher resolution and S/N observations are available.

As the binary components of CPD -59° 2635 are probably in synchronous rotation with the orbital period, we believe that the later spectral types (i.e. O8V and O9.5V respectively) are more realistic in describing each star in this binary system, being the earlier ones probably produced by photo-spheric heating on each star from its companion and/or the colliding wind region between the stars.

3.3 Physical Parameters

In what follows we will estimate the physical parameters of the binary components of CPD -59° 2635. We adopt for this star the visual magnitude and distance modulus of Trumpler 16 published by Massey & Johnson (1993), namely $V = 9.27$ and $M_v - V_0 = 12.55 \pm 0.08$, close to the value of $M_v - V_0 = 12.6$ obtained by Feinstein et al. (1973). Also from Massey & Johnson (1993), we take, for CPD -59° 2635, $E_{B-V} = 0.54$, $R = 3.2$ and thus $V_0 = 7.54$. In order to obtain individual absolute magnitudes, we need an estimate of the luminosity ratio of the binary components. We applied the corrected integrated-absorption method of Petrie (1940) in the way described by Niemela & Morrison (1988). We used equivalent widths measured for HeI 4387 and 4471 and HeII

4686 Å absorptions in spectra where those features are better resolved. We corrected for continuum overlapping using equivalent widths of the same lines measured for individual stars of similar spectral types, taken from Mathys, 1988. Then we calculated for each selected spectral line the quotient ($L_2/L_1 = \langle (B.K_a)/(A.K_b) \rangle$), where A is the equivalent width of the line measured in the spectrum of the most intense component, B is the equivalent width of the same line as observed in the weaker component, and $K_{a,b}$ are the equivalent widths measured for single stars of spectral types O8 V and O9 V, respectively. Performing these measurements in several spectra of CPD -59° 2635 observed near phases of maximum separation of the components we obtained an average value of $L_2/L_1 = 0.45 \pm 0.14$, which we have used in the following calculations. With this luminosity ratio and the adopted distance modulus, we obtained individual absolute magnitudes of $M_V = -4.61 \pm 0.1$ and -3.74 ± 0.1 for the primary and secondary components, respectively.

Our classification of the components of CPD -59° 2635 as O8 V and O9.5 V corresponds to $T_{\text{eff}} = 38450$ K and $BC = -3.68$ for the primary, and $T_{\text{eff}} = 34620$ K and $BC = -3.36$ for the secondary, according to the calibration of effective temperatures (T_{eff}) and bolometric corrections (BC) proposed by Vacca, Garmany & Shull (1996, hereafter VGS). However, according to Schmidt-Kaler (1982), the corresponding effective temperatures and bolometric corrections would be $T_{\text{eff}} = 35800$ K and $BC = -3.54$ for the primary, and $T_{\text{eff}} = 31500$ K and $BC = -3.25$ for the secondary. Therefore, depending on which calibration we adopt, we would find somewhat different values for the bolometric magnitudes, and thus, luminosities of each binary component.

Knowing the luminosities and effective temperatures, we can derive the radii of the stars, that we want to compare with the radii of the critical Roche lobes. Those were estimated using the expression given by Paczynski (1971):

$$r_1 \sin i = a \sin i (0.38 + 0.2 \log(M_1/M_2))$$

for a “mean” Roche radius of r_1 and separation a . We obtained individual Roche radii of $r_1 \sin i = 8.8 R_\odot$ and $r_2 \sin i = 7.8 R_\odot$. We need to know something about the inclination of the orbital plane in order to compare these critical Roche radii with the Stefan-Boltzmann radii of the stars.

The physical parameters derived for the binary components are summarized in Table 3.

Under the assumption that the system is in synchronous rotation (which seems reasonable in a massive binary of short period) we derived probable rotational velocities for its components (quoted in Table 3 which are higher than the observed rotational velocities of single stars of similar spectral types (e.g. Slettebak et al., 1975 ; Conti & Ebbets, 1977).

We tried to estimate the projected rotational velocities ($V \sin i$) comparing the observed absorption profiles of He I 4388 Å and 4471 Å with flux profiles from non-LTE model atmospheres by Auer & Mihalas (1972). We chose models corresponding to T_{eff} of 40000, 35000 and 30000 K and $\log g = 4$ to represent the binary components. The model profiles were convolved with different rotational velocity profiles, finding satisfactory agreement with observations for $V \sin i$ values of $180 \pm 25 \text{ km s}^{-1}$ and $140 \pm 30 \text{ km s}^{-1}$ for the primary and secondary components, respectively. Com-

Table 4. Three deep *ROSAT* HRI pointings which include CPD -59° 2635.

Sequence Identification	Begin Date	End Date	Exposure
RH900385N00	1992-07-31	1992-08-02	11527
RH900385A03	1994-07-21	1994-07-29	40555
RH202331N00	1997-12-23	1998-02-10	47095

paring these results with the calculated rotational velocities, we obtain, for the inclination of the orbital plane, values of 64° and 79° , for the primary and secondary, respectively, using the radii derived through the calibration by VGS, or 56° and 59° , for primary and secondary, respectively, using the calibration by Schmidt-Kaler (1982). However, the errors involved in the $V \sin i$ determination give room for a large range of inclinations.

Assuming the mass-spectral type relation for normal O-type stars by VGS (1996), we can expect masses near 25 and 21 M_\odot for the individual binary components of CPD -59° 2635. These values are similar to (or slightly larger than) those obtained from the observation of eclipsing binary systems with O8V and O9V components (e.g. EM Car, Andersen & Clausen, 1989; Y Cyg, Burkholder, Massey & Morrell, 1997; CQ Cep, Kartascheva & Svechnikov, 1989). This also points to an orbital inclination of $56^\circ \pm 6^\circ$, similar to the values estimated from the line widths. If these estimates are correct, the system is not likely to present eclipses. However, some kind of light variations may occur due to tidal deformation, considering that both components are hot luminous stars in a close binary system. Also, if our guess for the inclination is as supposed, the system would be detached, with both components within their critical Roche lobes, as we would expect for a young binary with non evolved components.

4 X-RAY EMISSION

CPD -59° 2635 was detected as a serendipitous X-ray source during numerous pointing in the Carina Nebula by the *ROSAT* X-ray satellite observatory with both the Position Sensitive Proportional Counter (PSPC) and the High Resolution Imager (HRI). In the PSPC images the star is unresolved from other nearby X-ray sources (notably the O stars HD 93343 and Tr 16 #182) due to the rather coarse spatial resolution of the PSPC ($\sim 1'$). The HRI has finer spatial resolution ($\sim 10''$) and so can better resolve CPD -59° 2635 from surrounding sources, providing a more accurate measure of the uncontaminated X-ray emission from the star. Table 4 lists 3 deep *ROSAT* HRI pointing which include CPD -59° 2635.

The source lies about $4.2'$ off axis, and at this position the 50% encircled energy radius is about $3''$. We extracted source counts from these 3 HRI sequences in an $8''$ region centered on CPD -59° 2635. We extracted background counts from a region of blank sky centered at $\alpha_{2000} = 10^h 45^m 19.6^s$, $\delta_{2000} = -59^\circ 44' 43.2''$ using an extraction radius of $40''$ to reduce the statistical uncertainty in the net rate.

Figure 6 shows the extracted net light curve for the

Table 3. Physical Parameters of CPD -59° 2635.

Calibration	Primary component		Secondary component	
	VGS	Schmidt-Kaler	VGS	Schmidt-Kaler
$T_{\text{eff}} [K]$	38450	35800	34620	31500
M_{bol}	-8.3 ± 0.15	-8.1 ± 0.15	-7.1 ± 0.15	-7.0 ± 0.15
$L [L_{\odot}]$	162000 ± 20000	143000 ± 20000	54000 ± 11000	49000 ± 11000
$R_{\text{S-B}} [R_{\odot}]$	9.1 ± 0.4	9.8 ± 0.4	6.5 ± 0.5	7.4 ± 0.5
$R_{\text{S-B}}/R_{\text{Roche-lobe}}$	0.8 ± 0.1	0.9 ± 0.1	0.7 ± 0.1	0.8 ± 0.1
$V_{\text{rot}} [km.s^{-1}]$	200 ± 10	215 ± 10	142 ± 15	164 ± 15

Notes: a) $R_{\text{S-B}}$ means Stefan-Boltzmann radii.

b) Theoretical Roche-lobe radii were desafected by the $\sin i$ factor using a probable average value for the inclination of the orbital plane, namely 60° .

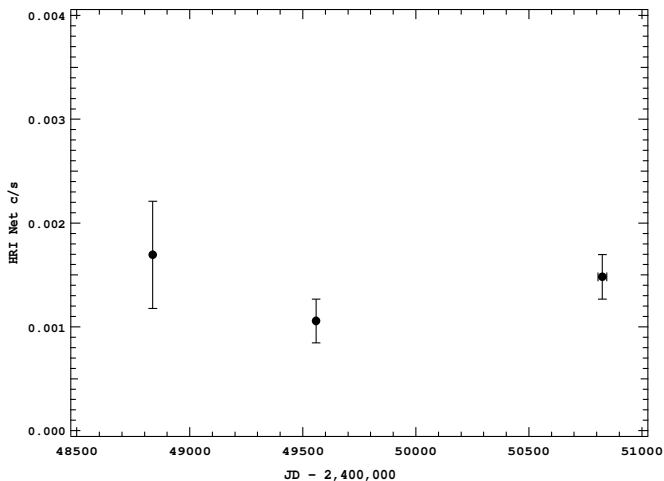


Figure 6. HRI X-ray light curve of CPD -59° 2635.

source. There is no evidence for variability. Because the HRI has no spectral resolution, we could not determine X-ray luminosity by direct spectral fitting. Rather, to determine the X-ray luminosity we converted the total net count rate to luminosity by assuming a Raymond-Smith thermal source spectrum with a temperature $kT = 0.5$ keV and an absorbing column $N_H = 2 \times 10^{21} \text{ cm}^{-2}$, which should reasonably approximate the X-ray emission from OB type stars in the Carina nebula. At $4'$ off-axis, the HRI vignetting correction is 1.01 (David, et al., 1997); the total net count rate, corrected for vignetting, is $1.35 \pm 0.14 \times 10^{-3}$ HRI counts s^{-1} . With our assumed spectral parameters, this corresponds to an X-ray luminosity $L_x = 3.8 \times 10^{31}$ ergs s^{-1} in the *ROSAT* band (0.2 – 2.4 keV), uncorrected for absorption, using $M_v - V_0 = 12.55$. After correcting for absorption, the X-ray luminosity at the source is approximately $L_{x,unabs} = 9 \times 10^{31}$ ergs s^{-1} in the *ROSAT* band. With a total bolometric luminosity $L_{\text{tot}} \sim 200000L_{\odot}$ the ratio of the unabsorbed X-ray luminosity to the total luminosity is $\log L_x/L_{\text{tot}} \sim -7$, similar to the canonical value of this ratio in the *ROSAT* band (Berghöffer et al. 1997). According to this, CPD -59° 2635 does not show excess in its X-ray flux compared to other O-type stars, and the question about why it looks brighter than its neighbour HD 93343 in the *ROSAT* HRI image of Figure 1 remains to be clarified when more observations of both stars are available.

5 CONCLUSIONS

In the present study we demonstrate that CPD -59° 2635 is a close binary system in a circular orbit. Both binary components are O-type stars, and the short period of binary motion suggests strong interactions between the stellar winds.

Variations of the order of one subclass in the spectral types of both components are observed, probably related to the phenomenon known as *Struve-Sahade effect*. A possible explanation for the Struve-Sahade effect, analyzed by Gies et al. (1997), is that it is present in systems expected to contain colliding winds with X-ray generation from the bow shock between the stars. However, the observed X-ray light curve does not show any significant variations, and moreover, the ratio L_x/L_{bol} seems to be similar to that observed for other O-type stars.

This star is a massive close binary, with hot, luminous components (O8V + O9.5V) and thus a good candidate for further exploration of colliding wind effects.

With the estimated inclination $\sim 60^{\circ}$, we can conclude that the stellar radii are smaller than the corresponding Roche lobes, the system being detached, as one would expect from the evolutionary status of a member in a cluster still containing unevolved O3 stars.

Though the system is not expected to present eclipses, future photometric studies could reveal the presence of phase locked light variations produced by tidal deformation of the binary components. This would provide the opportunity of making a better estimate of the inclination of the orbital plane, and consequently lead to the derivation of absolute individual masses for the components of CPD -59° 2635. No need to recall that this is of fundamental astrophysical interest concerning O-type stars.

6 ACKNOWLEDGEMENTS

We thank the director and staff of CASLEO for technical support and kind hospitality during the observing runs. N.I.M. is indebted to the director and staff of CTIO for the use of their facilities. We acknowledge use at CASLEO of the CCD and data acquisition system supported under U.S. NSF grant AST-90-15827 to R. M. Rich.

The Digitized Sky Survey in the southern hemisphere is based on photographic data obtained using The UK Schmidt Telescope. The UK Schmidt Telescope was operated by the Royal Observatory Edinburgh, with funding from the UK Science and Engineering Research Council, until 1988 June,

and thereafter by the Anglo-Australian Observatory. Original plate material is copyright the Royal Observatory Edinburgh and the Anglo-Australian Observatory. The plates were processed into the present compressed digital form with their permission. The Digitized Sky Survey was produced at the Space Telescope Science Institute under US Government grant NAG W-2166. This research has made use of NASA's Astrophysics Data System Abstract Service. This research has made use of data obtained from the High Energy Astrophysics Science Archive Research Center (HEASARC), provided by NASA's Goddard Space Flight Center. Useful discussions with R. Barbá are very much appreciated.

REFERENCES

- Andersen J., & Clausen J.V., 1989, *A&A*, 213, 183
Auer L. H., & Mihalas D. 1972, *Ap.J.S.*, 24, 193.
Berghöffer, T., Schmitt, J. H. M. M., Danner, R., and Cassinelli, J., 1997, *A&A*, 322, 167.
Burkholder V., Massey P. & Morrell, N.I., 1997, *ApJ*, 490, 328
Chlebowski, T., 1989, 342, 1091.
Chlebowski T., & Garmany C. D. 1991, *AJ*, 368, 241.
Chlebowski, T., Harnden, Jr., F. R., & Sciortino, S. 199, *ApJ*, 341, 427. David, L., et al., 1997, ROSAT High Resolution Imager Calibration Report, RSDC/SAO.
Conti P. S., & Burnichon M. L. 1975, *A&A*, 38, 467.
Conti P. S., & Ebbets, D. 1977, *ApJ*, 213, 438.
Corcoran M. F. 1999, *Rev Mex AASC*, 8, in press
David P., Goldwurm A., Murakami T., Paul J., Laurent P., Goldoni P. 1997, *A&A.*, 322, 229D.
Feinstein A., Marraco H. G., & Muzzio J. C. 1973, *A&AS.*, 12, 331.
Gies D. R., Bagnuolo W. G. Jr., & Penny L. R. 1997, *AJ*, 479, 408.
Jeffers H. M., van den Bos W.H., Greeby F. M. 1963, *Index Catalogue of Visual Double Stars*, Univ. California, Publ Lick Obs., Vol XXI.
Kartascheva T.A. & Svechnikov M.A., 1989, *Astrofiz. Issled. Izv. SAO*, 28, 3
Kerton C. R., Ballantyne D. R., & Martin P. G. 1999, *AJ*, 117, 2493.
Lafler J., & Kinman T. D. 1965, *ApJS*, 11, 199.
Levato H., & Malaroda S. 1982, *PASP*, 94, 807.
Massey P., & Johnson J. 1993, *AJ*, 1053, 980.
Mathys, G. 1988, *A&AS*, 76, 427.
Niemela, V. S., & Morrison, N. D. 1988, *PASP*, 100, 1436.
Packzynski B. 1971, *Ann. Rev. Astron. Astrphys.*, 9, 183.
Petrie, R.M. 1940, *Publ. Dom. Astroph. Obs. Victoria*, 7, 205.
Schmidt & Kaler 1982, in "Landolt-Börnstein, NS", Vol. 2, p. 455.
Slettebak A., Collins G. W., Boyce P. B., White N. M., & Parkinson T. D. 1975, *Ap.J.S.* 29, 137.
Stephenson C. B., & Sanduleak N. 1971, *Publ. Warner & Swasey Obs.*, 1, 1.
Stevens, I. R., Blondin, J. M., & Pollock, A.M.T., 1992, *ApJ*, 386, 265.
Usov, V. V., 1992, *ApJ*, 389, 635.
Vacca W. D., Garmany C. D. & Shull J. M. 1996, *ApJ*, 460, 914 (VGS)
Walborn N. 1982, *AJ*, 87, 1300.
Walborn N., & Fitzpatrick E. 1990, *PASP*, 102, 379.

This figure "figure1.jpg" is available in "jpg" format from:

<http://arxiv.org/ps/astro-ph/0105015v1>